Dynamics Analysis of the Rijke Tube Thermoacoustics

Mathematical Modeling using Luikov and Wave Equations with its Experimental Validation

I. Mejía Alonso
Thermoacoustics for Cooling
Engineering Center for Industrial Development
Querétaro, México
imejia@cidesi.edu.mx

E. E. Rodríguez Vázquez
National Research Laboratory for Cooling Technology
Engineering Center for Industrial Development
Querétaro, México
eloy.rodriguez@cidesi.edu.mx

C. A. Núñez Martín
Dynamic Optimization of Cooling Devices
Engineering Center for Industrial Development
Querétaro, México
canunez@posgrado.cidesi.edu.mx

L. A. Montoya Santiyanes
Rotordynamics for Cooling
Engineering Center for Industrial Development
Querétaro, México
lmontoya@posgrado.cidesi.edu.mx

H. J. Zúñiga Osorio
Flow Dynamics for Cooling
Engineering Center for Industrial Development
Querétaro, México
hzuniga@posgrado.cidesi.edu.mx

***Abstract*— This paper deals with the mathematical modeling for the thermoacoustic phenomena in a simple geometry combustion chamber represented as the Rijke tube. The methodology developed to get an analytical model from the Luikov equations for the dynamical behavior of both variables of interest the temperature and pressure distributions into the cited chamber is described briefly. Through this model, the time and space Eigenvalues are calculated to interpret them in terms of the combustion chamber geometry; also the spatial distribution (modal shapes or Eigenvectors) of both variables into the confined volume in the chamber are analyzed by the boundary conditions. The obtained analytical model from the Luikov modified equations is complemented with an experimental modeling for the dynamics of the same variables of interest, but based on the wave equation and considering the same boundary conditions. To validate both models for the thermoacoustics dynamics, a Rijke tube experiment was developed, by getting the experimental data to support the analytical hypothesis from the synthetized models. The main purpose of this paper is to compare the two mathematical modeling methodologies to know the set of assumptions needed to have a real idea of the fundamental modal shapes for the temperature and pressure in this combustion chamber geometry when the thermoacoustic phenomena is presented.**

Keywords-thermoacoustics; Rijke tube experiment; Luikov equations and wave equation.

NOMENCLATURE

X	: a dimensional Cartesian coordinate
T	: time
ρ	: density
T	: temperature
Q	: thermal energy
q	: acoustical perturbation
a_m	: diffusion coefficients for gases
a_q	: diffusion coefficients for temperature
C_q	: heat capacity
λ	: heat of phase change
ε	: ratio of vapor diffusion coefficient
k	: wavenumber
κ	: bulk modulus for the air
ξ	: displacement
P	: pressure
c	: sound speed in the medium
ω	: angular frequency

I. INTRODUCTION

Modern society needs to be conscience about all energy conversion process which affects the natural environment health. There are several efforts to maximize the natural energetic resources use by the synergy of thermodynamic technologies that combines systems for cooling and heating with several applications [1]. However, the achieved magnitude of both the worldwide population as well as the energy consumption for the ambient conditioning for living or for the perishables products conservation are considerable with the current natural energetic resources availability [2] [3].

In terms of the power generation technology which takes advantage from the synergy of two complemented thermodynamically cycles, we have the gas turbine technologies. The ammonia gas turbines combine the absorption ammonia cycle to diminish the surface temperature of the combustion chamber housing; then this transported energy heats the ammonia-air mixture to increase the combustion performance into the cited chamber [4]. This technology is applied for naval transportation where the ammonia use does not affect the population health and the engine performance is critical because of the fuel availability. In this context, the new trend for this technology is to apply it for the home services suppling using the industrial waste as fuel.

Other example of the synergy from a modified thermodynamic cycle is the heat pumps technology; which works based on the vapor compression so it complements several air conditioning systems and this device works in both directions to heat or cooling [5]. Nowadays, because of the time market availability this technology cannot be considered innovation but it is one of the most representative examples of efficiency in terms of the resources use for the ambient conditioning.

In the same technological synergy and because of its thermo-electrical nature Peltier's devices are used for the heating and cooling purposes. In these experimental cases, the energy transportation is mainly performed by conduction (not convection) [6], so their implementations are more punctually located in terms of energy transportation.

Cited technologies have been carefully designed to have the best thermodynamic performance in terms of the variables of interest listed as the temperature, energy and pressure; but these design engineering are based on the steady state behavior of the named variables, where the relationships between them do not considers the dynamical evolution of each one neither and their cross effects.

The thermoacoustic phenomena can be described as the acoustical energy caused from an uncontrolled density of heat in a confined volume [7]. In the gas turbine technology point of view, thermoacoustics means that the heat released in a combustion chamber generates pressure oscillations inside which decreases the engine performance, [8]. This relationship between heat and air pressure (sound waves) was discover by Rayleigh [9] and formulate by Merkli [10].

Thermoacoustic unstable evolution may cause several problems in the fuel system of a gas turbine, therefore it induces: efficiency degradation, premature wear of components and catastrophic failure [11]. Also, thermoacoustic phenomenon combined with the high levels of both pressures and temperatures affects the fuel air mixture process and then de combustion performance, producing also highly polluting particles such as NOx [12].

Nowadays, the state of the art concerned with the thermoacoustic phenomenon effects on the gas turbines performance, has been mainly focused on the development of some techniques as well as the swirling flows [13-14]. These swirling flows provide aerodynamic stability to the combustion process by producing regions of recirculating flows which diminish the flame length and increase the residence time of the reactants in the flame zone [14]. Experimental analysis from combustion test rig using different kind of injectors, constrictors, air-fuel mixes have been performed to find the best technique for combustion system [15]. Also, in terms of the flow, others studies have included premixed fluid and Helmholtz resonator [16].

The gas turbine combustion modelling and simulations, along with the acoustic phenomenon perturbation, implies the necessity of implementing a control algorithm. The basic gas turbine model equations [17] are important for analysis, design and simulation of control system, especially for Combined Cycle Power Plants (CCPP) [18] and [19].

Focusing on acoustics, new passive and active control techniques for such thermoacoustic instabilities have been developed and implemented [20] as well as techniques of: Adaptive Sliding Phasor Averaged Control (ASPAC: adaptation of the valve-commanded fuel phase for flow variations) [21] and Multiscale extended Kalman (MSEK: prediction of the time-delayed states) are promising techniques to reduce the energy consumption produced by pressure oscillations [22], nevertheless, more research is required.

In the same way, into the perturbation control topic, the dynamics model for the thermoacoustic phenomena proposed in this work has been envisaged to be the first part of a continuous control algorithm to diminish its effects into a combustion chamber. This research is carried out for the Engineering Center for Industrial Development (CIDESI) at Queretaro México, by the National Laboratory for Cooling Technologies Research (LaNITeF).

This paper structure has been defined to follow up the methodology proposed to validate a mathematical model for the thermoacoustic dynamics in a Rijke tube combustor; which consist in a theoretical modeling based on the Luikov equations adapted for the confined volume of the gas flowing in the cited chamber, and which is described in Section II. Then in Section III the procedure to develop the analytical model of pressure oscillation trough air columns is presented. Section IV presents the results from a Rijke tube experiment; here the required Fourier analysis is detailed to find the fundamental oscillation mode, where because of the prediction the speed of sound and the medium properties such as density, are required to determined parameter values of pressure distribution model. Section V describes the

results and validation of both theoretical and analytical models. Conclusions are presented in Section V.

II. THEORETICAL MODEL FOR THE TEMPERATURE AND PRESSURE DISTRIBUTION FROM THE LUIKOV EQUATIONS

Luikov proposed a model for the heat and mass transfer in capillary porous bodies at 1966 [23], which mainly consist in a differential equation system of first order with two degrees of freedom (temperature and mass). This model has been modified several times as an alternative model from the Navier – Stokes equation [24] when its analytics solutions are needed for flow dynamics through different kinds of medias [25] [26] and [27].

A. Analitical solution of the Luikov equations

Originally the Luikov equations were developed for the mass and energy transportation through porous bodies; but in this case, the confined volume into the combustion chamber is not a solid media neither a porous one. Therefore, the hypothesis to use this equation system is based on the concept of finite volume, where the mass transportation does not face an interface between them; it just does at the boundary conditions. The heat transportation between the finite volumes is no considered, because the energy transportation is done mainly by convection.

Then the Luikov model is defined by a first order differential equation system, for temperature and pressure as well as it is:

$$\begin{aligned}\frac{\partial T(t,x)}{\partial t} &= a_q \frac{\partial^2 T(t,x)}{\partial x^2} + \frac{\lambda\varepsilon}{C_q}\frac{\partial \rho(t,x)}{\partial t} + a_1 Q(t,x)\\ \frac{\partial \rho(t,x)}{\partial t} &= a_m \frac{\partial^2 \rho(t,x)}{\partial x^2} + a_m \delta \frac{\partial^2 T(t,x)}{\partial x^2} + a_2 q(t,x)\end{aligned} \tag{1}$$

where T and ρ are the temperature and air density respectively, Q is the thermal energy supplied and q the acoustical perturbation. a_m and a_q are the diffusion coefficients for the air density and temperature. If it is considered that the physical properties, which define the coefficients of (1), are constants and executing the substitution of the first order timed differential for the air density magnitude, equation (1) becomes

$$\begin{aligned}\frac{\partial T(t,x)}{\partial t} &= A_1 \frac{\partial^2 T(t,x)}{\partial x^2} + A_2 \frac{\partial^2 \rho(t,x)}{\partial x^2} + B_1 Q(t,x) + B_2 q(t,x)\\ \frac{\partial \rho(t,x)}{\partial t} &= A_3 \frac{\partial^2 T(t,x)}{\partial x^2} + A_4 \frac{\partial^2 \rho(t,x)}{\partial x^2} + B_3 q(t,x)\end{aligned} \tag{2}$$

Another significant consideration in this proposal is that all function can be separable from the time domain to the space domain, so dimensional functions can be taken as

$$\begin{aligned}T(t,x) &= f(t)g(x)\\ \rho(t,x) &= p(t)h(x)\\ Q(t,x) &= r(t)c(x)\\ q(t,x) &= q(t)\end{aligned} \tag{3}$$

then (2) takes the form of:

$$\begin{aligned}g(x)\frac{df(t)}{dt} &= A_1 f(t)\frac{d^2 g(x)}{dx^2} + A_2 p(t)\frac{d^2 h(x)}{dx^2} + B_1 r(t)c(x) + B_2 q(t)\\ h(x)\frac{dp(t)}{dt} &= A_3 f(t)\frac{d^2 g(x)}{dx^2} + A_4 p(t)\frac{d^2 h(x)}{dx^2} + B_3 q(t)\end{aligned} \tag{4}$$

By defining the next list of matrices

$$\begin{aligned}\mathbf{F}(t)_{2\times 2} &= \begin{bmatrix} f(t) & 0 \\ 0 & p(t)\end{bmatrix}_{2\times 2} \quad \mathbf{G}(x)_{2\times 2} = \begin{bmatrix} g(x) & 0 \\ 0 & h(x)\end{bmatrix}_{2\times 2}\\ \mathbf{R}(t)_{2\times 2} &= \begin{bmatrix} r(t) & 0 \\ 0 & q(t)\end{bmatrix}_{2\times 2} \quad \mathbf{C}(x)_{2\times 2} = \begin{bmatrix} c(x) & 0 \\ 0 & 1\end{bmatrix}_{2\times 2}\\ \mathbf{A}_{2\times 2} &= \begin{bmatrix} A_1 & A_2 \\ A_3 & A_4\end{bmatrix}_{2\times 2} \quad \mathbf{B}_{2\times 2} = \begin{bmatrix} B_1 & B_2 \\ 0 & B_3\end{bmatrix}_{2\times 2}\end{aligned} \tag{5}$$

equation (3) can be organized as:

$$\mathbf{G}(x)\frac{d}{dt}\mathbf{F}(t)\begin{bmatrix}1\\1\end{bmatrix} = \mathbf{A}\frac{d^2}{dx^2}\mathbf{G}(x)\mathbf{F}(t)\begin{bmatrix}1\\1\end{bmatrix} + \mathbf{BC}(x)\mathbf{R}(t)\begin{bmatrix}1\\1\end{bmatrix} \tag{6}$$

The theory for the dynamics analysis for systems is focused on the analysis of the impulse response, because it represents the system transient response when it changes from an equilibrium state (Transfer Function). Therefore, to analyze this system dynamics, it is considered that there is not heat injection (energy source) neither pressure perturbation

$$\mathbf{G}(x)\frac{d}{dt}\mathbf{F}(t)\begin{bmatrix}1\\1\end{bmatrix} = \mathbf{A}\frac{d^2}{dx^2}\mathbf{G}(x)\mathbf{F}(t)\begin{bmatrix}1\\1\end{bmatrix} \tag{7}$$

The different domains functions can be now separated from (7); therefore, by equating them to a constant parameter which has almost the same interpretation than the wave number concept

$$\begin{aligned}\frac{1}{f(t)}\frac{d}{dt}f(t) &= \left[\frac{1}{g(x)}\right]\left[A_1\frac{d^2}{dx^2}g(x) + A_2\frac{d^2}{dx^2}h(x)\right] = -k_1^2\\ \frac{1}{p(t)}\frac{d}{dt}p(t) &= \left[\frac{1}{h(x)}\right]\left[A_3\frac{d}{dx}g(x) + A_4\frac{d}{dx}h(x)\right] = -k_2^2\end{aligned} \tag{8}$$

It is shown that the referred equality constants are the time domain Eigenvalues, from

$$\frac{d}{dt} f(t) + k_1^2 f(t) = 0 \qquad \lambda_f = -k_1^2 \qquad f(t) = c_1 e^{-k_1^2 t}$$
$$\frac{d}{dt} p(t) + k_2^2 p(t) = 0 \qquad \lambda_p = -k_2^2 \qquad p(t) = c_2 e^{-k_2^2 t} \tag{9}$$

Into the space domain, the analytical solution needs to solve the next differential equations system

$$A_1 \frac{d^2}{dx^2} g(x) + A_2 \frac{d^2}{dx^2} h(x) + k_1^2 g(x) = 0$$
$$A_3 \frac{d^2}{dx^2} g(x) + A_4 \frac{d^2}{dx^2} h(x) + k_2^2 h(x) = 0 \tag{10}$$

which can be simplified as

$$[A_2 A_3 - A_1 A_4] \frac{d^4}{dx^4} h(x) - [A_1 k_2^2 + A_4 k_1^2] \frac{d^2}{dx^2} h(x) - k_1^2 k_2^2 h(x) = 0$$
$$[A_2 A_3 - A_1 A_4] \frac{d^4}{dx^4} g(x) - [A_1 k_2^2 + A_4 k_1^2] \frac{d^2}{dx^2} g(x) - k_1^2 k_2^2 g(x) = 0 \tag{11}$$

The special Eigenvalues from (11) are imaginaries, as it is easier shown next

$$C_1 \frac{d^4}{dx^4} h(x) + C_2 \frac{d^2}{dx^2} h(x) + C_3 h(x) = 0$$
$$C_1 \frac{d^4}{dx^4} g(x) + C_2 \frac{d^2}{dx^2} g(x) + C_3 g(x) = 0$$

where

$$\alpha_{1,2} = \frac{-C_2 \pm \sqrt{C_2^{\,2} - 4C_1C_3}}{2C_1} \quad \Rightarrow \quad \lambda_{x1,x2} = \pm j\sqrt{\alpha_1}, \quad \lambda_{x3,x4} = \pm j\sqrt{\alpha_2} \tag{12}$$

Then the especial solution is given by

$$g(x) = c_3 \cos(\sqrt{\alpha_1} x) + c_4 \sin(\sqrt{\alpha_1} x) + c_5 \cos(\sqrt{\alpha_2} x) + c_6 \sin(\sqrt{\alpha_2} x)$$
$$h(x) = c_7 \cos(\sqrt{\alpha_1} x) + c_8 \sin(\sqrt{\alpha_1} x) + c_9 \cos(\sqrt{\alpha_2} x) + c_{10} \sin(\sqrt{\alpha_2} x) \tag{13}$$

B. Rijke boudary conditions

The next step to get the analytical solution is to calculate the constants in terms of the boundary conditions, so if it is considered the ambient temperature and air density as the reference for the first boundary condition of the Rijke tube shown in Fig. 1, then the constants for the dual dominium solution functions given by

$$T(t,x) = b_1 e^{-k_1^2 t} \cos(\sqrt{\alpha_1} x) + b_2 e^{-k_1^2 t} \sin(\sqrt{\alpha_1} x) + b_3 e^{-k_1^2 t} \cos(\sqrt{\alpha_2} x) + b_4 e^{-k_1^2 t} \sin(\sqrt{\alpha_2} x)$$
$$\rho(t,x) = b_5 e^{-k_2^2 t} \cos(\sqrt{\alpha_1} x) + b_6 e^{-k_2^2 t} \sin(\sqrt{\alpha_1} x) + b_7 e^{-k_2^2 t} \cos(\sqrt{\alpha_2} x) + b_8 e^{-k_2^2 t} \sin(\sqrt{\alpha_2} x) \tag{14}$$

result on

$$T(0,0) = 0 = b_1 + b_3 \qquad b_3 = -b_1$$
$$\rho(0,0) = 0 = b_5 + b_7 \qquad b_7 = -b_5 \tag{15}$$

The Rijke tube setup consist just in an open tube vertically oriented, in this case the longitude of this tube is L and the thermal energy is punctual supplied along the axial direction at $x=L/5$ (see Fig. 1).

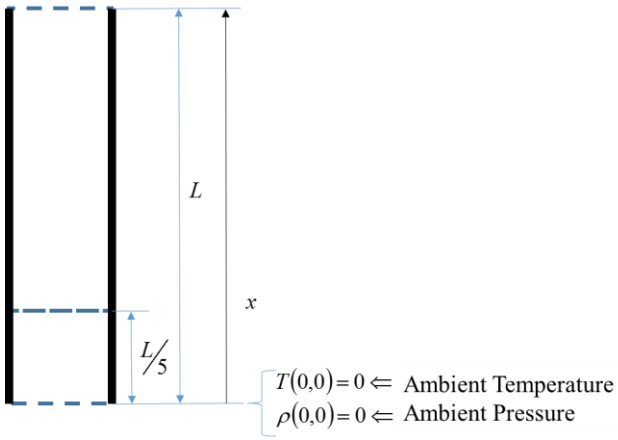

Figure 1. First boundary condition of the Rijke tube.

The second set of coefficients are calculated by considering also the second boundary condition of the Rijke tube (see Fig. 2), as

$$b_1 = -\frac{\left(b_2 \sin(\sqrt{\alpha_1} L) + b_4 \sin(\sqrt{\alpha_2} L)\right)}{\cos(\sqrt{\alpha_1} L) - \cos(\sqrt{\alpha_2} L)} = \frac{b_2 \sin(\sqrt{\alpha_1} L) + b_4 \sin(\sqrt{\alpha_2} L)}{\cos(\sqrt{\alpha_2} L) - \cos(\sqrt{\alpha_1} L)}$$
$$b_5 = -\frac{\left(b_6 \sin(\sqrt{\alpha_1} L) + b_8 \sin(\sqrt{\alpha_2} L)\right)}{\cos(\sqrt{\alpha_1} L) - \cos(\sqrt{\alpha_2} L)} = \frac{b_6 \sin(\sqrt{\alpha_1} L) + b_8 \sin(\sqrt{\alpha_2} L)}{\cos(\sqrt{\alpha_2} L) - \cos(\sqrt{\alpha_1} L)} \tag{16}$$

Here the entire solution can be simplified as

$$T(t,x) = e^{-k_1^2 t} \left[\frac{b_2 \sin(\sqrt{\alpha_1} L) + b_4 \sin(\sqrt{\alpha_2} L)}{\cos(\sqrt{\alpha_2} L) - \cos(\sqrt{\alpha_1} L)} \left(\cos(\sqrt{\alpha_1} x) - \cos(\sqrt{\alpha_2} x)\right) + b_2 \sin(\sqrt{\alpha_1} x) + b_4 \sin(\sqrt{\alpha_2} x) \right]$$
$$\rho(t,x) = e^{-k_2^2 t} \left[\frac{b_6 \sin(\sqrt{\alpha_1} L) + b_8 \sin(\sqrt{\alpha_2} L)}{\cos(\sqrt{\alpha_2} L) - \cos(\sqrt{\alpha_1} L)} \left(\cos(\sqrt{\alpha_1} x) - \cos(\sqrt{\alpha_2} x)\right) + b_6 \sin(\sqrt{\alpha_1} x) + b_8 \sin(\sqrt{\alpha_2} x) \right],$$

and their spatial derivation are given by

$$\frac{\partial T(t,x)}{\partial x} = e^{-k_1^2 t}\left[\frac{b_2\sin\left(\sqrt{\alpha_1}L\right)+b_4\sin\left(\sqrt{\alpha_2}L\right)}{\cos\left(\sqrt{\alpha_2}L\right)-\cos\left(\sqrt{\alpha_1}L\right)}\left(\sqrt{\alpha_2}\sin\left(\sqrt{\alpha_2}x\right)\right.\right.$$
$$\left.\left.-\sqrt{\alpha_1}\sin\left(\sqrt{\alpha_1}x\right)\right)+\sqrt{\alpha_1}b_2\cos\left(\sqrt{\alpha_1}x\right)+\sqrt{\alpha_2}b_4\cos\left(\sqrt{\alpha_2}x\right)\right]$$

$$\frac{\partial \rho(t,x)}{\partial x} = e^{-k_2^2 t}\left[\frac{b_6\sin\left(\sqrt{\alpha_1}L\right)+b_8\sin\left(\sqrt{\alpha_2}L\right)}{\cos\left(\sqrt{\alpha_2}L\right)-\cos\left(\sqrt{\alpha_1}L\right)}\left(\sqrt{\alpha_2}\sin\left(\sqrt{\alpha_2}x\right)\right.\right.$$
$$\left.\left.-\sqrt{\alpha_1}\sin\left(\sqrt{\alpha_1}x\right)\right)+\sqrt{\alpha_1}b_6\cos\left(\sqrt{\alpha_1}x\right)+\sqrt{\alpha_2}b_8\cos\left(\sqrt{\alpha_2}x\right)\right] \quad (17)$$

The third boundary condition of the Rijke tube is located at point in which the thermal energy is supplied. Therefore, the temperature has a maximum point there while the air density is minimal. These boundary conditions are illustrated in Fig. 3. With these considerations the third set of coefficient are estimated as:

$$b_2 = -Db_4$$
$$b_6 = -Db_8 \quad (18)$$

where

$$D = \frac{\left(\sin\left(\sqrt{\alpha_2}L\right)\left(\sqrt{\alpha_2}\sin\left(\sqrt{\alpha_2}\frac{L}{5}\right)-\sqrt{\alpha_1}\sin\left(\sqrt{\alpha_1}\frac{L}{5}\right)\right)+\left(\cos\left(\sqrt{\alpha_2}L\right)-\cos\left(\sqrt{\alpha_1}L\right)\right)\sqrt{\alpha_2}\cos\left(\sqrt{\alpha_2}\frac{L}{5}\right)\right)}{\left(\sin\left(\sqrt{\alpha_1}L\right)\left(\sqrt{\alpha_2}\sin\left(\sqrt{\alpha_2}\frac{L}{5}\right)-\sqrt{\alpha_1}\sin\left(\sqrt{\alpha_1}\frac{L}{5}\right)\right)+\left(\cos\left(\sqrt{\alpha_2}L\right)-\cos\left(\sqrt{\alpha_1}L\right)\right)\sqrt{\alpha_1}\cos\left(\sqrt{\alpha_1}\frac{L}{5}\right)\right)}$$

Given the final model version as:

$$T(t,x) = b_4 e^{-k_1^2 t}\left[\frac{\sin\left(\sqrt{\alpha_2}L\right)-D\sin\left(\sqrt{\alpha_1}L\right)}{\cos\left(\sqrt{\alpha_2}L\right)-\cos\left(\sqrt{\alpha_1}L\right)}\left(\cos\left(\sqrt{\alpha_1}x\right)\right.\right.$$
$$\left.\left.-\cos\left(\sqrt{\alpha_2}x\right)\right)+\sin\left(\sqrt{\alpha_2}x\right)-D\sin\left(\sqrt{\alpha_1}x\right)\right] = b_4 e^{-k_1^2 t} f_x(x)$$

$$\rho(t,x) = b_8 e^{-k_2^2 t}\left[\frac{\sin\left(\sqrt{\alpha_2}L\right)-D\sin\left(\sqrt{\alpha_1}L\right)}{\cos\left(\sqrt{\alpha_2}L\right)-\cos\left(\sqrt{\alpha_1}L\right)}\left(\cos\left(\sqrt{\alpha_1}x\right)\right.\right.$$
$$\left.\left.-\cos\left(\sqrt{\alpha_2}x\right)\right)+\sin\left(\sqrt{\alpha_2}x\right)-D\sin\left(\sqrt{\alpha_1}x\right)\right] = b_8 e^{-k_2^2 t} f_x(x) \quad (19)$$

Both variables distributions along the axial longitude are the same; but, as well as it was discussed before, the temperature $T_L(t)$ at $x=L/5$ is maxima, and through convection with a controlled energy source $Q_L(t)$ coefficient b_4 can be written as:

$$b_4 = \frac{1}{f_x\left(\frac{L}{5}\right)}\left(T_L(t)-\frac{a_1}{k_1^2}Q_L(t)\right)e^{k_1^2 t} \quad (20)$$

In this point the temperature behavior can be written in terms just of b_4 as

$$T(t,x) = \frac{1}{f_x\left(\frac{L}{5}\right)}\left(T_L(t)-\frac{a_1}{k_1^2}Q_L(t)\right)\left[\frac{\sin\left(\sqrt{\alpha_2}L\right)-D\sin\left(\sqrt{\alpha_1}L\right)}{\cos\left(\sqrt{\alpha_2}L\right)-\cos\left(\sqrt{\alpha_1}L\right)}\left(\cos\left(\sqrt{\alpha_1}x\right)\right.\right.$$
$$\left.\left.-\cos\left(\sqrt{\alpha_2}x\right)\right)+\sin\left(\sqrt{\alpha_2}x\right)-D\sin\left(\sqrt{\alpha_1}x\right)\right] \quad (21)$$

By taking advantage of the equivalent axial distribution of both variables of interest, the b_8 coefficient can be considered as:

$$b_8 = b_4\frac{\rho(t,x)e^{k_2^2 t}}{T(t,x)e^{k_1^2 t}} = b_4\frac{\rho\left(t,\frac{L}{5}\right)}{T\left(t,\frac{L}{5}\right)}\frac{e^{k_2^2 t}}{e^{k_1^2 t}} \quad (22)$$

Finally, the dynamics of the spatial behavior of both estimation variables can be written in terms of the boundary conditions and the energy supplied to the Rijke tube.

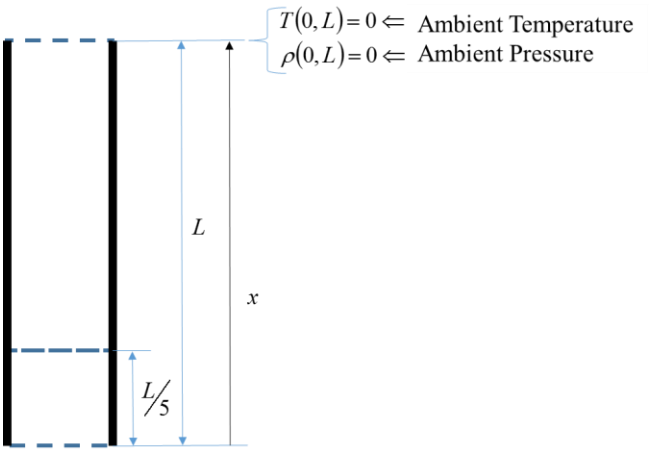

Figure 2. Second boundary condition of the Rijke tube.

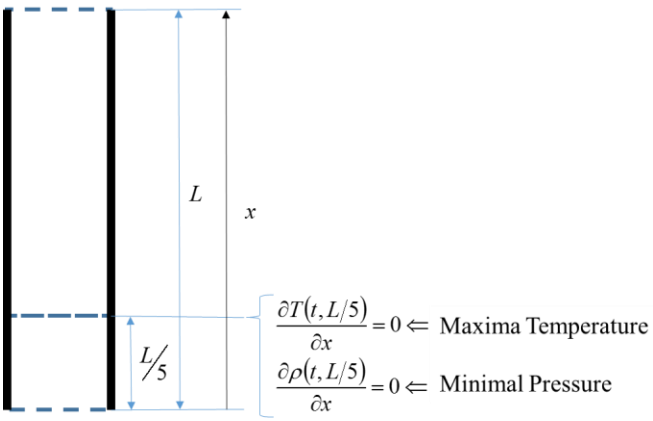

Figure 3. Thrid boundary condition of the Rijke tube.

Here we can say that because of the constant volume, the air density and pressure variables have the same dynamical and spatial behavior.

III. ANALYTICAL MODEL FOR PRESSURE OSCILLATION FROM THE WAVE EQUATION

Thermoacoustic phenomenon is defined as the direct transformation from thermal energy into acoustic energy. Three conditions are required for this transformation [1]:

1. The medium must be a compressible fluid,
2. A temperature gradient must exist, and
3. The control volume must be contained by a physical border (chamber housing) [28].

The wave equation is a linear second-order differential equation for both the time as spatial domains, which describes the propagation of oscillations in a continuous media. The goal of this section is to establish a wave equation relation for the pressure variable in an air column when the thermoacoustic phenomena appears into a Rijke tube.

A. Stationary wave in an air column

The wave equation for acoustic pressure is given by [29].

$$\frac{\partial^2 \xi}{\partial t^2} = \frac{\kappa}{\rho_0}\frac{\partial^2 \xi}{\partial x^2} \tag{23}$$

with ξ the displacement in the air, κ the bulk modulus for the air and ρ_0 the air density under equilibrium conditions.

As well as it was performed for the Luikov equations, the wave equation solution for the acoustic was solved via the variables separation strategy.

The concept of a standing wave is based on the spatial superposition of two waves with the same time and space frequencies, which travel in opposite directions in the medium with the same amplitude. For this Rijke tube experiment, the standing wave resulting from the wave equation for the air behavior, which is given as

$$\xi(x,t) = 2\xi_0 \sin(kx)\cos(\omega t) \tag{24}$$

where k index does correspond to the wavenumber, ξ_0 is the wave amplitude and ω its angular frequency. The Taylor law for fluid gradient [30] was used to formulate the pressure of standing waves in an air column, where

$$p - p_o = \kappa\frac{\partial \xi}{\partial x}; \tag{25}$$

therefore, the pressure behavior can be written as

$$P(x,t) = -2\xi_0 \kappa k \cos(kx)\cos(\omega t) \tag{26}$$

Equation (26) describes the distribution of pressures with no boundary conditions. Then again, as well as it occurs for the Luikov equation solutions, the boundary conditions for the air wave describes the Eigenvectors, which for this case are analyzed as nodes (see Fig. 4).

B. Node analysis (modal shapes or Eigenvectors)

A tube open at both ends provides a physical border for the concerned air column contained. Reflection causes nodes and antinodes of pressure and air displacement, as well as it is illustrated by Fig. 4.

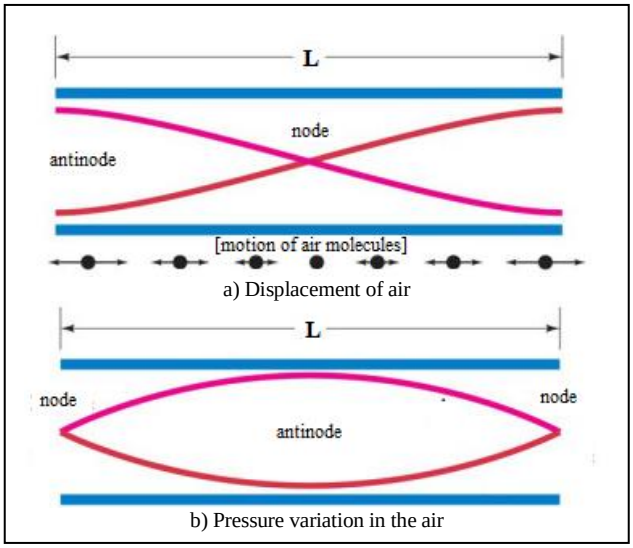

Figure 4. Pressure and displacement for the air in the columns.

Air displacement nodes are associated with the motion of its molecules, which produce in this case the modal nodes. Therefore, at both ends of the column into the Rijke tube boundaries must be a pressure node because the atmosphere cannot present a significant pressure change induced by this phenomena [31]. Then the relationship between pressure and motion of the air can be written as (24).

The generalized one-dimensional equation that describes the pressure distribution of an air contained in a cylindrical combustion chamber is obtained by considering the boundary conditions illustrated on Figs. 1 and 2. Then from (24), the pressure distribution model can have been formulated:

$$P(x,t) = -2\kappa k\xi \cos(k(x + \pi/2k))\cos(\omega t) \tag{27}$$

from the boundary conditions evaluation, the obtained model coefficients are:

Condition 1:

$$\begin{aligned} P((0),t) &= -2\kappa k\xi \cos(k((0) + \pi/2k))\cos(\omega t) \\ 0 &= \cos(\pi/2)\cos(\omega t) \\ 0 &= 0 \end{aligned}$$

Condition 2:

$$\begin{aligned} P((L),t) &= -2\kappa k\xi \cos(k((\pi/k) + \pi/2k))\cos(\omega t) \\ 0 &= \cos(3\pi/2)\cos(\omega t) \\ 0 &= 0 \end{aligned}$$

So the one-dimension pressure distribution model on the can combustor results [1].

$$P(x,t) = -2kc^2 \rho\xi \cos(k((\pi/k) + \pi/2k)) \cos(\omega t) \quad (28)$$

IV. RIJKE TUBE EXPERIMENTE

With the intention of confirming, thermoacoustic is concerned with the interactions between heat (thermos) and pressure oscillations in gases (acoustics). Then a "Rinke Tube", named after its inventor, is a fundamental tool for studying thermoacoustic phenomenon. Rijke tube turns heat into sound, by creating a self-amplifying standing wave. This open cylinder resonator contains a metallic copper mesh positioned about one-fifth of the total tube length. When the mesh is heated by a burner flame and then when the flame is take out, the concerned mesh will produce a strong sound pitch at its resonant frequency for several seconds.

A Rijke tube experiment was performed considering the experimental setup shown in Fig. 5 [32]. This Rijke tube consist on: a steel pipe of 0.5 m long and a 0.04445 m (1 ¾ in) diameter with a thickness of 0.00121 m, is selected and instrumented, as seen in Fig. 5. Let x_m be the distance (0.12m) where metallic mesh was placed.

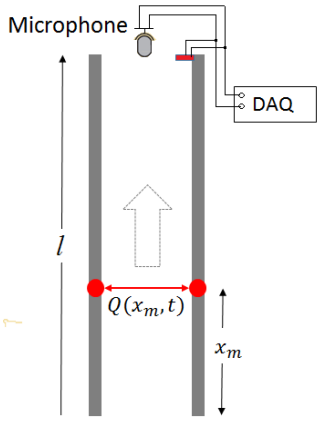

Figure 5. Data adquisition for Rijke tube experiment .

Rijke tube turns heat into sound, by creating a self-amplifying standing wave just after the heat source provided by a gas burner was taken out. Gas burner add energy to the system until to metallic mesh rise a 600 °C of temperature; then, the heat source is moved aside and thermoacoustic phenomenon appears. It is important to consider that the position of pipe must be maintained vertical.

A. *Fourier analysis*

Time domain analysis is the interpretation of physical signals evolution with respect to time. It is beneficial when observing data such as temperature. However, because of the time response some applications require analyzing the frequency components of signals, such as pressure oscillation of the air.

The acoustic pressure was measured using a microphone during Rijke tube experiment [33]. Time domain acoustic signal does not provide significant information for analysis. Hence, Fourier analysis is required. A fast Fourier transform (FFT) is an algorithm that samples a signal in time domain (or space domain) and turns it into frequency domain, exhibiting its frequency components. FFT helps to find the fundamental frequency produced by the air column resonance.

The experiment is executed taking 44100 samples per second using the microphone. The Fast Fourier Transform was applied with a resolution of 15 bits. Frequency resolution is 1.34 Hz, i.e., every 743 ms the algorithm takes a package sample to analyze.

The signal for amplitude in time domain and frequency domain obtained with the microphone is shown in Fig. 6. Here the first modal mode presence is identified at 301 Hz with an amplitude of 0.1941 Pa.

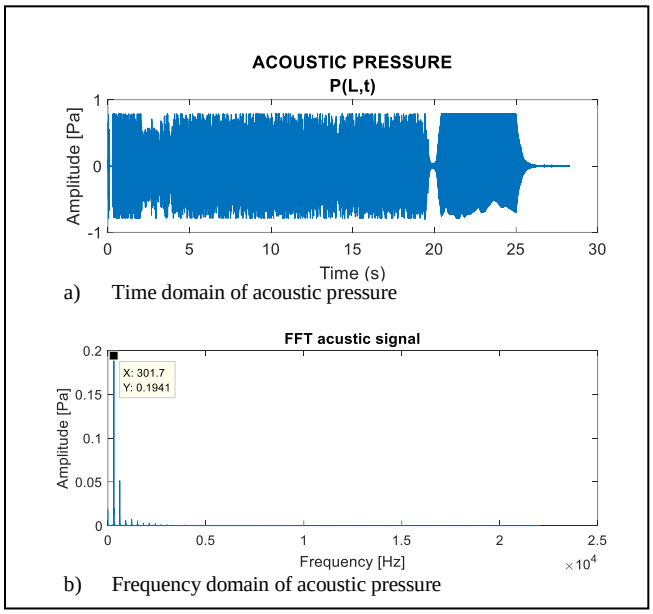

Figure 6.Signal analysis of acoustic pressure

B. *Sound speed in the air*

The speed of sound is affected by changes in the medium (density, humidity, temperature, etc.). For our study case, the element that changed significantly is the temperature.

The geometry of the combustor determines frequency and wavelength of the oscillating pressure produced by the thermoacoustic effect. The symbol λ is the label for length of the wave. Fig. 7 illustrates a reflection wave on the pipe open ends. The output wave (green) and the reflected wave (red) only perform half a cycle each. The tube length is half the Wavelength.

Considering idealistic conditions, the fundamental frequency is inversely proportional to the length of the tube.

$$c/2\pi\acute{\imath}=f \quad (29)$$

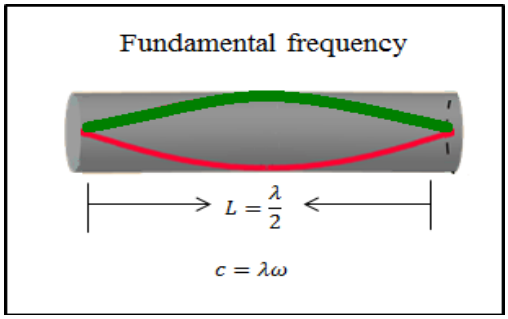

Figure 7. First vibration mode in air column.

In an ideal tube, the wavelength of the sound produced is directly proportional to the length of the tube. A tube with aperture at one end and closed at the other one produces sound with a wavelength equal to four times the length of the tube. In acoustics, end correction factor is a short distance added to the actual length of a resonance pipe, to calculate the precise resonance frequency of the pipe. The tone of a real tube is lower than the predicted theoretically. The end correction for a pipe is given as

$$\lambda = 2(L + 0.61D) \tag{30}$$

At the end, the speed of sound resulted is 379.18 m/s.

C. Temperature of the air

Temperature is a physical quantity produced by motion of the molecules, giving a perception of hot and cold. Temperature is associated with friction. Molecular friction is associated with pressure and density in the air. The ideal gas law is a good approximation of the behavior of many gases under several conditions, although it has limitations. The most frequently form of a state equation is given by

$$\frac{P}{\rho} = \frac{RT}{M} \tag{31}$$

The acoustic wave velocity c depends of the material properties. Speed of sound is proportional to bulk modulus and inversely proportional to density of the air as dictate in (23), resulting in this case as

$$\frac{\kappa}{\rho} = c^2$$

Where $\kappa = \gamma P$ and γ is the heat capacity ratio. There is a strong relationship between pressure of the air, density of the air, temperature of the air and speed of sound [33]. This relationship is

$$\frac{\gamma P}{\rho} = c^2 = \frac{\gamma RT}{M} \tag{32}$$

Equation (32) implies that temperature can be expressed in terms of speed of sound.

$$T_{air} = \left(\frac{c_{air}}{20.055 \frac{m}{s \cdot K^{1/2}}} \right)^2 \tag{33}$$

Equation (33) is defined using nominal values of air. The density of a substance is the relationship between mass amount and volume occupied. The density can change by changing either the pressure or the temperature. Increasing the temperature generally decreases the density.

Table I shows the density of the air in terms of air temperature.

TABLE I. TEMPERATURE AND DENSITY OF THE AIR

Speed of sound (m/s)	T (K)	T(°C)	ρ [Kg/m^3]
379.18	357.48	84.48	0.9870

V. RESULTS

The one-dimension pressure distribution model on the concerned can-combustor is formulated on Section III, along with the determination of parameters' values.

$$P(x,t) = -2kc^2 \rho\xi \cos(k((\pi/k) + \pi/2k)) \cos(\omega t)$$

Pressure distribution along the can-combustor is described in Fig. 8. This paper becomes useful for several combustor chambers with similar geometries.

Advanced FFT Spectrum Analyzer is used to verify in real-time the signal evolution, as depicted in Fig. 9. Due to expansion and compression ratio, the air will generate high pressure areas whose magnitude is directly proportional to the temperature of the medium. The temperature of the metal gauze oscillates around 600 °C at t=0, convectively transferring the thermal energy and change the properties of the medium. The average temperature of the column was 78 ° C.

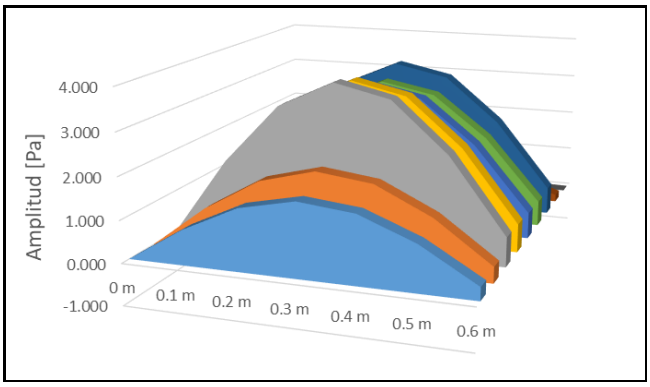

Figure 8. Fundamental mode of vibration in air column.

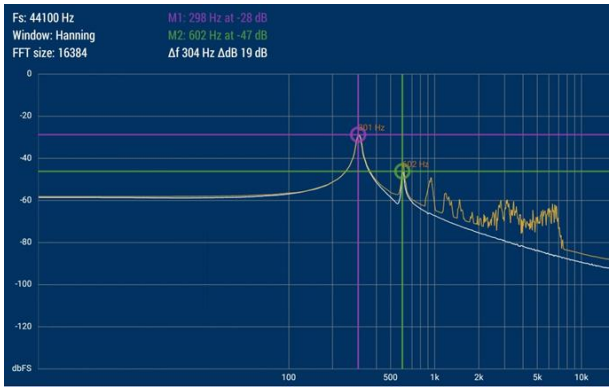

Figure 9. Fundamental frecuency measure on Rijke tube experiment.

It is experimentally proven with the results that the speed of sound has been altered by the temperature change in the medium that propagates the disturbance, which was 379 m/s. Following the relationship on (23), the fundamental frequency of the gaseous fluid contained in a cylindrical geometry is obtained. Thermoacoustic phenomenon presence is used to validate the pressure distribution model for the air oscillation inside the Rijke tube.

VI. CONCLUSION

Taking as reference theoretical results from equations (19) and (28) both predicts a modal node just at the middle of the Rijke tube axial dimension for the air density and pressure, respectively. Also, (19) predicts an antinode for the temperature behavior.

Experimentally, the air density and pressure modal node have been proven by the results reported in Fig. 8; where the thermodynamics relationship between the air flow speed (sound) and the internal temperature measured supports these results from the Eigenvalues gotten in Fig. 9.

So that, at the end, the main conclusion is that the propagation of acoustic oscillation in a compressive medium (air in this case) may be induced by applying thermal energy to the chamber housing surface, so the thermodynamic relationship between pressure, density and temperature has been verified for a single geometry combustor chamber, a Rijke tube in this case.

The pressure distribution model for the dynamic behavior of the pressure oscillation into a Rijke tube synthesized from the wave and Luikov equations, was validated by predicting the first mode frequency of the air column pressure inside, as well as it is shown in Fig. 10, where also the Fourier Analysis results are included.

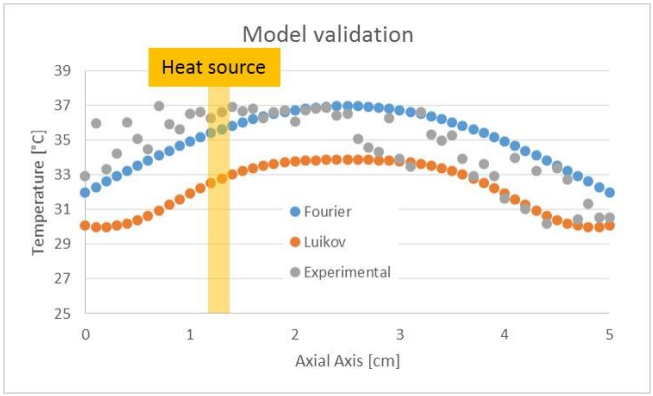

Figure 10. Experimental Model validation.

Experimental results illustrated in Fig. 10 were obtained by using a thermos-camera and a set of thermocouples at the Rijke tube external surface. Both models in the temperature space shows an acceptable prediction, but analysis needs to explain why boundary conditions has change in their average values.

Based on the temperature results, the Luikov equation for pressure can be used with certain reliability to have a model for both variables.

The next step is to use both models to predict the concerned variables behavior but by been taking into account the experimental measurement of their boundary values.

For the National Laboratory of Cooling Technology Research, the results reported here are important in terms of the thermoacoustic technology development to provide an alternative for the cooling systems; because from these fundamentals both models are going to be used to develop control strategies for the cooling generation and ambient conditioning.

For the P02 project from the CEMIE Eolic program, these results take importance because of the presence of the thermoacoustic phenomena in several additive manufacturing process, which disturbs the manufacturing finishing and composition.

ACKNOWLEDGMENT

Authors thanks National Council for Science and Technology (CONACYT) for the scholarships of the postgraduate students involved; also because of the support through the consolidation project for the National Laboratory Research on Cooling Technologies (LaNITeF) Budget No. 293784. These results were gotten by the synergy of both projects the LaNITeF consolidation as well as the P02 of the Mexican Center for Innovation in Eolic Energy (CEMIE Eólico) supported also by the Secretariat of Energy, through the Budget for Sustainable Energy.

REFERENCES

[1] I. Mejia, E.E. Rodriguez, C. Núñez and C. Cruz, “Thermoacoustics Analysis in a Rijke Tube,” The Thirteenth International Conference on Systems (ICONS 2018) IARIA, Apr. 2018, ISBN: 978-1-61208-626-2, ISSN: 2308-4243.

[2] M. Brauer, "Ambient Air polution Expousre Estimation for the Global Burden of Disease 2013," Enrimental Science & Technoloy, No. 50, pp. 79-88, 2016.

[3] GBD 2013 Risk Factors Collaborators, "Global, Regional, and Natural Comparative Risk Assessment of 79 Behavioral, Enviromental and Occupational, and Metabolic Risk or Clusters of Risks in 188 Countries, 1990 – 2013: A Systematic Analysis for the Global Burden of Disease Study 2013," The Lancet 394, pp. 2287 – 2323, 2016.

[4] A. Valera-Medina, S. Morris, J. Runyon, D.G. Pugh, R. Marsh, P. Beasley, T. Hughes, "Ammonia, Methane and Hydrogen for Gas Turbines," Energy Procedia, vol. 75, pp. 118 – 123, 2015.

[5] Y. Okuri, Heat pump type air conditioner, US patent, US5937669A, 1998.

[6] L. E. Bell, "Cooling, Heating, Generating Power, and Recovering Wasted Heat with Thermoelectric Systems," Science, vol. 321, Issue 5895, pp. 1457 – 1461, 2008.

[7] G. W. Swift, "Thermoacoustics; A Unifying Perspective for Some Engines and Refrigerators," Ed. Springer, ISBN: 978-3-319-66933-5, 2017.

[8] B. Schuermans, F. Güthe, D. Pennell, C. O. Paschereit, "Thermoacoustic Modelin of a Gas Turbine Using Transfer Function Measured Unde Full Engine Pressure," Journal of Engineering for Gas Turbine and Power, vol. 132, No. 11, 2010.

[9] J.W.S. B. Rayleigh, "The theory of sound," Book, vol. 2, London: Macmillan and Co. Cambridge 1877.

[10] P. Merkli and H Thomann, "Termoacoustic effects in a resonance tube," Journal of Fluid Mechanics, vol. 70, Cambridge University. July 1975.

[11] T. C. Lieuwen and V. Yang, "Combustion Instabilities in Gas Turbine Engines: Operational Experience, Fundamental Mechanisms and Modeling," American Institute of Aeronautics and Astronautics, 2006.

[12] M. O. Vigueras-Zuñiga, A. Valera-Medina, N. Syred, and P. Bowen, "High Momentum Flow Region and Central Recirculation Zone Interaction in Swirling Flows," Sociedad Mexicana de ingeriera Mecanica. vol. 4, pp. 195-204, 2014.

[13] S. Hochgreb, D. Dennis, and I. Ayranci, "Forced and Self-Excited Instabilities From Lean Premixed, Liquid-Fuelled Aeroengine Injectors at High Pressures and Temperatures" Turbine Technical Conference and Exposition, ASME Turbo Expo 2014.

[14] N. Yadav and A. Kushari. "Effect of swirl on the turbulent behaviour of a dump combustor flow", Journal of Aerospace Engineering, vol. 224, no. 6, pp. 705-717, 2010.

[15] A. Valera, A. Griffiths, and N. Syred, "Analysis of the Impact Caused by Coherent Structures in Swirling Flow Combustion Systems", Ingeniería investigación y Tecnología, FI-UNAM, 2012.

[16] Z. Zhang, D. Zhao, N. Han, S. Wang, J. Li, "Control of combustion instability with a tunable Helmholtz resonator", Aerospace Science and Technology, Elsevier, 2014.

[17] W. Rowen. "Simplified mathematical representations of heavy-duty gas turbines", ASME J. Eng. Power, vol. 105, pp. 865-869, 2013.

[18] J. Rai, N. Hasan, B. Arora, R. Garai, R. Kapoor and Ibraheem. "Performance Analysis of CCGT Power Plant using MATLAB/Simulink Based Simulation", International Journal of Advancements in Research & Technology, vol. 2, no. 5, 2013.

[19] R. Smith, J. Ranasinge, C. Gulen, Combined Cycle Power Plant, US Patent, US20070017207A1, 2005.

[20] T. Samad and A. Annaswamy. "The impact of Control Technology", [Online] Available: ww.ieeecss.org, 2011

[21] A. Banaszuk, "Control of Combustion Inestability: From Passive to Active Control of Combustors", Grand Challenges for Control, IEEE, 2012.

[22] A. V. Luikov, Heat and mass transfer in capillary porous bodies, Pergamon Press, Oxford, U.K., 1966.

[23] P. Contantin, C. Fioas, Navier – Stokes Equations, The University of Chicago Press, ISBN 0-226-11548-8, 1989.

[24] D. De-Vries, Simultaneous transfer of heat and moisture in porous media, Transaction on Am. Geophy, Unio 39, pp. 909-016, 1968.

[25] T.Z. Harmathy, Simultaneous moisture and heat transfer in porous systems with particular reference of drying, I. Ec. Fundamentals, vol. 8, no. 1, pp. 92 – 103, 1969.

[26] K.N. Shukla, Diffusion Process During Dryling of Solid, World Scientific Publishing Co., Singapore, 1993.

[27] C. Dong, K. Jay, and J. Yong. "Analysis of the combustion instability of a model gas turbine combustor by the transfer matrix method", Journal of Mechanical Science and Technology, vol. 23, April, pp. 1602-1612, 2009.

[28] S. Kai-Uwe, K. Rainer and B. Hans-Jörg. "Experimental Characterization of Premixed Flame Instabilities of a Model Gas Turbine Burner". Flow, Turbulence and Combustion, vol. 76, no. 2, pp. 177-197, 2006.

[29] M. Alonso and E. Finn, "Physical: Waves and Fields" Book, vol. II. Fondo Educativo Interamericano, pp 694-712.

[30] Universidad de Valladolid, "Waves and propagation", Curso online:https://www.lpi.tel.uva.es/~nacho/docencia/ing_ond_1/trabajos_05_06/io2/public_html/viento/principios_viento.html. April 2017.

[31] S. Shariati, A. Franca, B. Oezer, R. Noske, D. Abel, A. Brockhinke, "Modeling and Model Predictive Control of Combustion Instabilities in a Multi-section Combustion Chamber Using Two-Port Elements", IEEE Multi-conference on Systems and Control, Antibes, France. 2014

[32] Y. Cengel and M. Boles, "Termodinamica" Book, 7th Edition, Mc Graw Hill, 2012.

[33] J. Mathews and F. Kurtis. "Numerical Methods Using Matlab". Fourth Edition. Prentice Hall New Jersey. Chapter 2, 2004.

[34] E. Gutiérrez, G. Vélez, D. Szwedowicz, J. Bedolla, C. Cortés. "Identification of Close Vibration Modes of a Quasi-Axisymmetric Structure: Complemetary Study," Ingeniería Investigación y Tenología, vol XIV, Apr, pp. 207-222, 2012.